

Crystal Structure of Chlorinated Thiazine-Indigo

Jin Mizuguchi and Takatoshi Senju

Graduate School of Engineering, Yokohama National University
Hodogaya, Yokohama, Japan

Abstract

Thiazine-indigos are novel hydrogen-bonded, yellow to red pigments currently developed by Clariant. Commercially available chlorinated derivative (THI), for example, exhibits vivid red in the solid state while only pale yellow in solution. Structure analysis of THI has therefore been carried out in order to elucidate the color generation mechanism on going from solution to the solid state. THI is found to crystallize in space group $P\bar{1}$ with $Z = 1$. The molecule is entirely planar characterized by C_i symmetry. There are chains of intermolecular N–H...O hydrogen bonds on the molecular plane. The present intermolecular hydrogen bonds hold the molecules firmly together, leading to a high light and heat stability of THI as well as low solubility in solvents. The color change from yellow to red upon crystallization has been interpreted as arising mainly from intermolecular interactions between transition dipoles.

Introduction

Thiazine-indigos belong to a new class of hydrogen-bonded pigments currently developed by Clariant.¹ These compounds exhibit a variety of shades from yellow to red, depending on the substituents. The basic chromophore is quite similar to that of indigo and thioindigo. Fig. 1 shows the molecular structure of the chlorinated derivative (Pigment Red 279; abbreviated to THI) that has newly appeared on the market. As is typical of hydrogen-bonded pigments such as indigos, quinacridones and diketopyrrolopyrroles,² there are two pairs of N–H and C=O groups necessary for the formation of N–H...O intermolecular hydrogen bonds. The present H-bond network is assumed to cause the very good thermal and solvent resistance of THI.

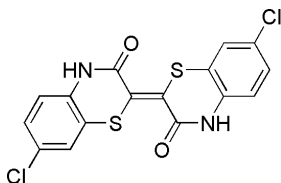


Figure 1. Molecular structure of chlorinated thiazine-indigo (THI).

Although THI exhibits a vivid red color in the solid state, it appears pale yellow in solution. This obviously indicates that the intermolecular interaction in the solid state is responsible for the drastic color change upon crystallization. For this reason, an attempt was made in the present investigation to clarify the crystal structure in order to elucidate the color generation mechanism of THI.

Experimental

Powdered THI was obtained from Clariant and purified by sublimation, using a two-zone furnace.³ Single crystals were then grown from solution in dimethylsulfoxide in an autoclave. The evaporated thin films were prepared onto glass substrates using a Tokyo Vacuum EG-240 under high vacuum. The evaporated films were exposed to acetone vapor for several hours to bring about the rearrangement of the molecules.

X-ray diffraction data on single crystals were collected on a Rigaku R-Axis RAPID-F diffractometer with $\text{CuK}\alpha$ radiation ($\lambda = 1.5419 \text{ \AA}$) at 93 K. The structure was solved by direct methods with Shelxs-86⁴ and refined by full-matrix least squares on F^2 using teXsan program package.⁵ X-ray diffraction diagrams of evaporated THI were measured with a Rigaku RINT 2000. UV-vis spectra were recorded on a Shimadzu UV-2400PC spectrophotometer. Polarized reflection spectra were measured on single crystals by means of a Carl Zeiss UMSP 80 microscope-spectrophotometer.

Semi-empirical MO calculations were made for absorption bands using the INDO/S Hamiltonian by Quantum CAChe Ver.3.2 for Microsoft Windows.⁶

Results and Discussion

Structure Analysis. Table 1 lists the crystallographic parameters for THI.⁷ The space group is $P\bar{1}$ and the crystal system is triclinic. Fig. 2 shows the ORTEP plot for THI. The molecule belongs to the point group of C_i and is entirely planar.

Figures 3 and 4 show the projection of the crystal structure onto the (b,c) plane as well as the molecular arrangement along the stacking axis. On the molecular plane, there are chains of intermolecular hydrogen bonds along the b -axis between the NH group of one molecule

and the O atom of the neighboring one. The present N–H...O hydrogen bonds form a two dimensional H-bond network as found in diketopyrrolopyrroles⁸ and quinacridone pigments.^{9,10} The N/O distance and the NH/O angle are 2.832 Å and 170°, respectively. Judging from the H-bond distance and angle, the THI H-bond is assumed to be stronger than that of indigo¹¹ (N/O: 2.862 Å and 132°), but weaker as compared with that of γ -quinacridone⁹ and diketopyrrolopyrroles⁷ (N/O: 2.756 Å and 163°; N/O: 2.825 Å and 175°). Another characteristic nature of the THI H-bond is the existence of small steps by about 0.57 Å between two molecules on the molecular plane as shown in Fig. 4. This kind of steps have also been recognized in 2,9-dimethylquinacridone¹⁰ as well as in modifications I and II of dithioketopyrrolopyrroles.^{12,13} Figure 5 shows the molecular overlap of two molecules A and B shown in Fig. 4. Close atomic contacts along the stacking axis are designated by dotted circles.

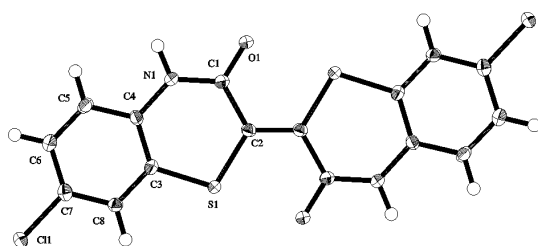


Figure 2. ORTEP plot of THI (50% probability).

Table 1. Crystallographic parameters⁷

Formula	$C_{16}H_8Cl_2N_2O_2S_2$
Crystal system	triclinic
Space group	$P\bar{1}$
Z	1
Molecular weight	395.28
a (Å)	4.5934(6)
b (Å)	7.83033(8)
c (Å)	10.403(1)
α (°)	92.040(9)
β (°)	99.38(1)
γ (°)	94.19(1)
V (Å ³)	367.8
T (K)	93
R_1	0.031

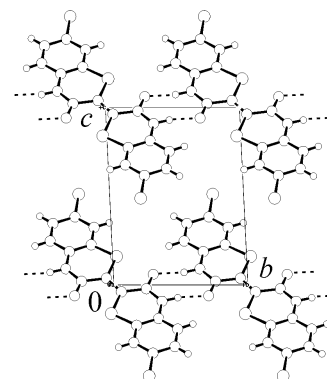


Figure 3. Projection of the crystal structure onto the (b,c) plane. The dotted lines denote intermolecular N–H...O hydrogen bonds.

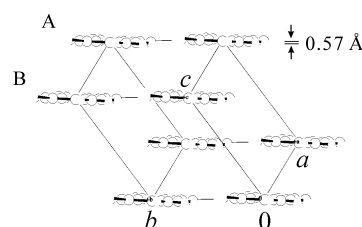


Figure 4. Side view of the two-dimensional H-bond network with a small step by about 0.57 Å.

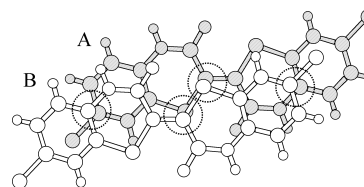


Figure 5. Molecular overlap of molecules A and B along the stacking axis. Close atomic contacts are designated by the dotted circles.

Solution Spectrum

Figure 6 shows the solution spectrum in dimethylsulfoxide for THI. The direction of the transition dipole based on MO calculations is also presented as a dotted line in the inset. Two intense bands appear at about 430 and 450 nm (molar extinction coefficient: about 13,400), accompanied by two additional absorption shoulders around 400 and 480 nm. On the other hand, the spectroscopic calculations shown in Table 2 suggest only one absorption band is expected to appear in the visible region. This evidently indicates that the longest-wavelength band around 480 nm is assigned to a pure electronic band as denoted by the 0–0 transition, to which one, or two or three vibrational transitions of about 1700 cm^{-1} are coupled to give the 0–1, 0–2 and 0–3 vibronic bands, respectively.

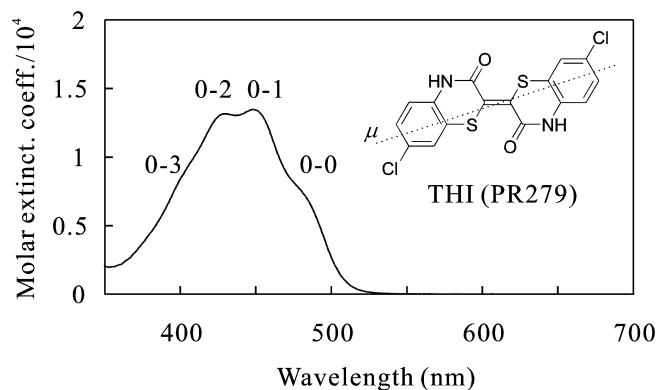


Figure 6. Solution spectrum in dimethylsulfoxide for THI. Molecular structure of THI is shown as an inset. The dotted line denotes the calculated transition dipole (μ).

Table 2. Calculated Absorption Bands and Their Oscillator Strength for THI Using the INDO/S Hamiltonian.

λ (nm)	Oscillator strength
386.9	0.73
268.1	0.12
230.1	1.06

Solid-state Spectra and X-ray Diffraction Diagrams in Evaporated Films

Figure 7 shows the solid-state spectra of evaporated THI before and after vapor treatment, together with the solution spectrum in dimethylsulfoxide. The spectral shape of the solution spectrum is quite similar to that of evaporated THI before vapor treatment, although one additional band is recognized in the longest-wavelength in the solid state (ca. 524 nm: band A). In fact, except band A, one-to-one correspondence of the absorption bands is well established between the two absorption spectra in solution and in the solid state. Evidently, band A is assigned as a new band that has appeared upon crystallization and is due to intermolecular interactions. In addition, band A is further displaced, due to vapor treatment, toward longer wavelengths by about 13 nm and intensified. The present spectral change is well correlated with the molecular rearrangement due to vapor treatment as described below.

Figure 8 shows the X-ray diffraction diagrams of evaporated THI before and after vapor treatment. The broad diffraction band around $2\theta = 26.5^\circ$ is due to the glass substrate used. The halo diffraction diagram before vapor treatment is rather indicative of an amorphous phase, although the H-bond network based on N-H...O is already present in this state as shown by a separate IR experiment. Then, vapor treatment brings about a diffraction peak around $2\theta = 27.5^\circ$ (interplanar distance: 3.3 Å), indicating that the molecules are ordered along the stacking axis. This implies that the spectral change is obviously caused by the ordering of the molecules along the stacking axis.

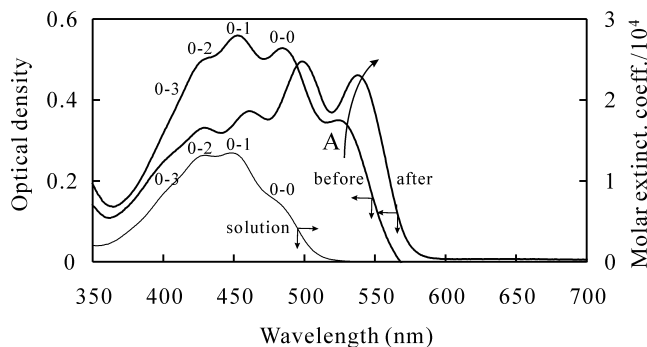


Figure 7. Solution spectrum and solid state spectra of evaporated THI before and after vapor treatment. (The film thickness: ca. 1000 Å)

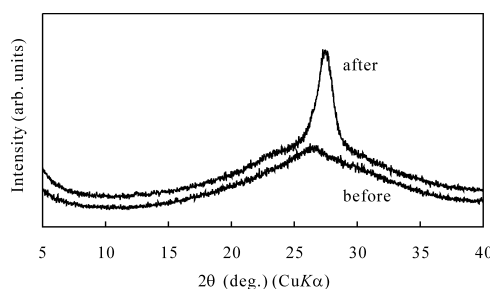


Figure 8. X-ray diffraction diagrams of evaporated THI before and after vapor treatment.

Temperature Dependence of Absorption Spectra in Evaporated Films

The temperature dependence of the absorption spectra sometimes serves as a good measure for the involvement of intermolecular interactions in the optical absorption. Crystal lattice is significantly contracted at low temperatures, leading to the enhancement of intermolecular interactions. Therefore, the absorption band arising from intermolecular interactions (i.e., band A in Fig. 6) is assumed to exhibit an appreciable temperature dependence at low temperatures.

Figures 9(a) and 9(b) show, respectively, the temperature dependence of the absorption spectra of evaporated THI before and after vapor treatment, measured in the temperature range between 20 and 300 K. Before vapor treatment, band A shows a moderate but still more significant temperature dependence as compared with that of the molecular bands as denoted by 0-0, 0-1, 0-2 and 0-3. On the other hand, as shown in Fig. 9(b), band A is apparently quite temperature dependent, indicating that the intermolecular interaction is greatly enhanced because of the molecular rearrangement due to vapor treatment. Then, an important question arises as to the origin of intermolecular interactions. In other words, what kind of intermolecular interactions are responsible for the appearance of band A? To this question, we answer in the following way. Since the molar extinction coefficient of THI (which is proportional to the square of the transition dipole) is very large (about 13,400) and the crystallinity is

greatly improved due to vapor treatment, it is highly probable that the resonance interaction between transition dipoles will occur to cause a bathochromic or hypsochromic shift to appear.¹⁴ The present excitonic consideration will also be borne out by polarized reflection spectra measured on single crystals as described below.

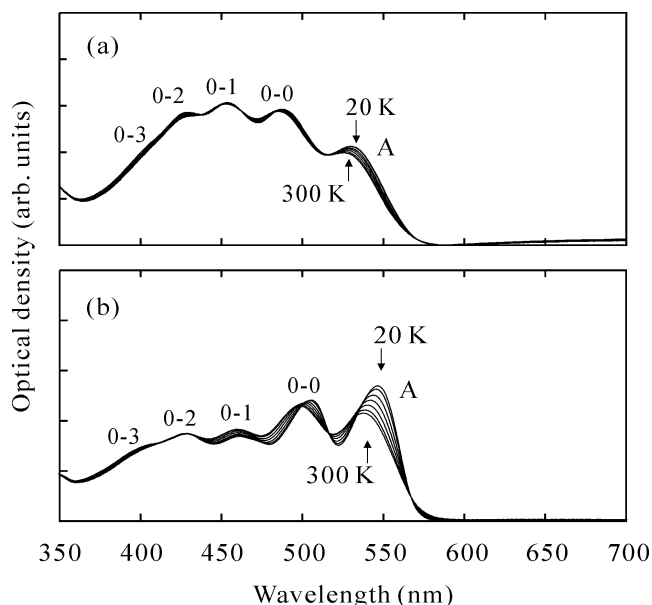


Figure 9. Temperature dependence of the absorption spectra of evaporated THI (a) before and (b) after vapor treatment.

Polarized Reflection Spectra Measured on Single Crystals

Figure 10 shows the polarized reflection spectra measured on the (100) plane of THI single crystals together with its projection. An intense reflection band appears at about 550 nm, accompanied by two small bands around 500 and 470 nm, for polarization parallel to the long-crystal axis. This is the direction of the calculated transition dipole (μ) as denoted by the broken line in Fig. 10(b). On the other hand, these bands are completely quenched for polarization perpendicular to the long-crystal axis. The appearance and disappearance of all reflection bands for different polarizations clearly indicate that there is only one single electronic transition in the visible region and that the direction of the transition dipole points along the long molecular axis. This is in good agreement with the result of MO calculations.

As seen in Fig. 10(b), the transition dipoles are almost aligned on the (*b,c*) plane in a fashion nearly “head-to-tail”. This greatly contributes to the bathochromic shift from 480 to 550 nm upon crystallization due to the resonance interactions between transition dipoles.¹⁴ Similar bathochromic displacements due to excitonic interactions are also observed in organic pigments such as diketopyrrolopyrroles¹⁵ and dicarboxyimide perylenes.¹⁶

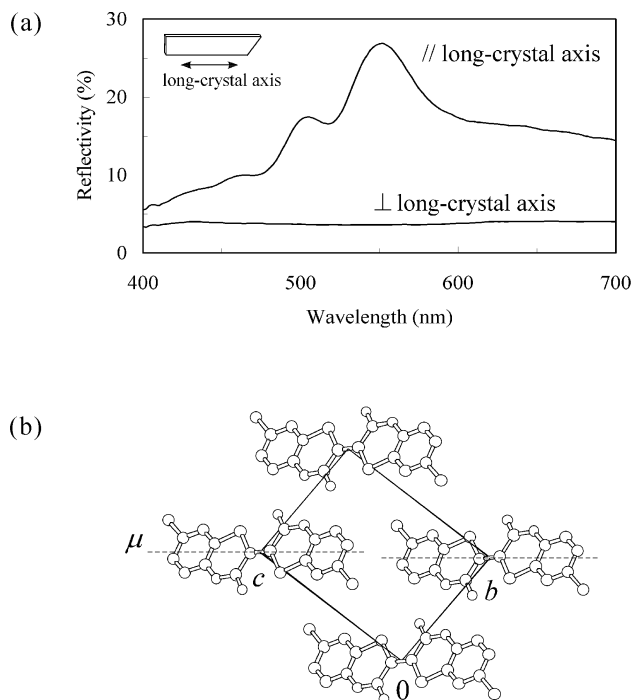


Figure 10. (a) Polarized reflection spectra for THI measured on the (100) plane. (b) Projection of the crystal structure onto the (*b,c*) plane. The broken line denotes the direction of the calculated transition dipole (μ).

Diffuse Reflectance Spectrum Measured on Powders

Figure 11 shows the diffuse reflectance spectrum measured on powdered THI. The position of the absorption bands as well as the whole spectral shape are quite similar to that of the polarized reflection spectra measured on single crystals and also to that of the absorption spectrum of evaporated THI after vapor treatment. Furthermore, the X-ray diffraction diagram of powdered THI confirms that the phase in powders coincides with that of single crystals.

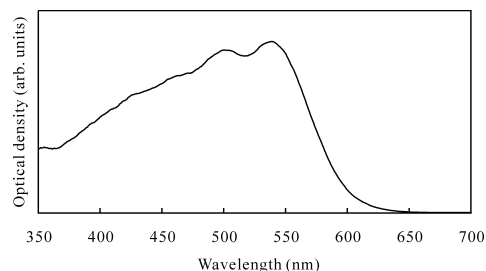


Figure 11. UV-vis diffuse reflectance spectrum for powdered THI.

Conclusions

THI is found to crystallize in space group $P\bar{1}$ and the molecule belongs to C_i symmetry. The molecular skeleton is entirely planar. There exists a two-dimensional N–H...O hydrogen bond network on the molecular plane characterized by small steps by about 0.57 Å on the molecular plane. The molecules are stacked with an appreciable overlap along the a -axis. The large spectral shift on going from solution to the solid state can most ly be attributed to the interaction between transition dipoles arranged in a fashion “head-to-tail” on the molecular plane.

References

1. M. U. Schmidt, Crystal engineering of benzimidazolone-dioxazine, thiazine-indigo and related pigments: From single crystals and powders over mixed crystals and solid solutions to supramolecules, *Proc. COLORCHEM 2000*, L6 (2000).
2. W. Herbst and K. Hunger, *Industrial Organic Pigments*, 2nd Ed., VCH, Weinheim, 1997.
3. J. Mizuguchi, *Cryst. Res. Technol.*, **16**, 695 (1981).
4. G. M. Sheldrick, *Acta Crystallogr.*, **A46**, 467 (1990).
5. teXsan. Ver. 1.11, Rev. 1., MSC and Rigaku (2001).
6. Quantum CAChe Ver. 3.2, Fujitsu Ltd. (1999).
7. T. Senju and J. Mizuguchi, *Z. Kristallogr. NCS*, **218**, 129 (2003).
8. J. Mizuguchi, A. Grubenmann, G. Wooden and G. Rihs, *Acta Crystallogr.*, **B48**, 696 (1992).
9. J. Mizuguchi, T. Sasaki and K. Tojo, *Z. Kristallogr. NCS*, **217**, 249 (2002).
10. J. Mizuguchi, T. Senju and M. Sakai, *Z. Kristallogr. NCS*, **217**, 525 (2002).
11. P. Süsse, M. Steins and V. Kupcik, *Z. Kristallogr.*, **184**, 269 (1988).
12. J. Mizuguchi, A. C. Rochat and G. Rihs, *Acta Crystallogr.*, **C46**, 1899 (1990).
13. J. Mizuguchi, M. Arita and G. Rihs, *Acta Crystallogr.*, **C47**, 1952 (1991).
14. M. Kasha, *Spectroscopy of the Excited State*, Plenum Press, NY, 1976, pg. 337.
15. J. Mizuguchi, *J. Phys. Chem. A*, **104**, 1817 (2000).
16. J. Mizuguchi and K. Tojo, *J. Phys. Chem. B*, **106**, 767 (2002).

Biography

Takatoshi Senju received his B.S. and Ph.D. degrees in Chemistry from the University of Tokyo in 1992 and 1997, respectively. Since then he worked in the Development and Engineering Research Center at Mitsubishi Chemical Co. in Okayama, Japan and then moved to Yokohama National University as Assistant Professor in 1999. His research interest includes synthetic and computational organic chemistry and electronic characterization of organic pigments. He is a member of the Chemical Society of Japan and the American Chemical Society. E-mail: tsenju@ynu.ac.jp